Journal of Science and Technology in Civil Engineering, HUCE, 2024, 18 (2): 149–162

PROBABILISTIC SAFETY ASSESSMENTS OF TRUSS STRUCTURES DESIGNED BY AISC 360-16 AND EC 3

Nhu Son Doan[a,*]

[a]*Faculty of Civil Engineering, Vietnam Maritime University,*
Room 902 A6 Building, No. 484 Lach Tray street, Le Chan district, Haiphong, Vietnam

Article history:
Received 15/12/2023, Revised 11/3/2024, Accepted 29/3/2024

Abstract

In globalization, the selection of the specifications for design practices depends on the investment agency. For example, steel truss structures can be designed using various codes, such as AISC 360-16 or EC 3. Although most specifications have recently been written in the limit state design approaches, which codes resulting in reasonable design solutions are rarely investigated. This work carried out reliability analyses to evaluate the probabilistic safety levels of the solutions designed by the abovementioned codes. Following the two design codes, two truss structures are first designed to satisfy the strength limit states. Various live-to-dead load ratios are also adopted for designing tension and compression members of the trusses. Afterward, Monte Carlo simulations are implemented to assess the failure probability of each design solution. Because the two codes are written in the limit state design formats, and the factors specified in the codes are established based on reliability frameworks, consistency and uniformity of the design solutions are investigated. It is revealed that the trusses designed with AISC 360-16 result in higher probabilistic safety levels compared with those using EC 3. However, the failure probability for tension and compression bars is more consistently obtained for those designed by EC 3. Moreover, the reliability indexes for tension bars are lower than those for compression members, regardless of the code used.

Keywords: reliability analysis; fully probabilistic analysis; Monte Carlo simulation; truss structure; AISC 360-16; EC 3.

https://doi.org/10.31814/stce.huce2024-18(2)-11

1. Introduction

Recently, design codes in America and Europe have been written in the limit state design (LSD) formats wherein components and connections of structures are classified as safe if they satisfy all limit states predefined in the codes. The load and resistance factors or partial safety factors specified in the codes are mostly determined based on a semi-probabilistic approach [1–3]. In the design practices, the members and connections are verified using the factors specified in the codes, and no probabilistic calculation is required; hence, LSD is classified as a semi-probabilistic approach [1]. In this way, the methods of LSD outperform the traditional method of allowable working stress because their partial safety factors are determined via the reliability-based approach, and the design process can be executed in the same way as the allowable working stress method. The design equation can be written as Eq. (1) for the design resistance R_d and the design load Q_d. The equal sign in Eq. (1) indicates the limit state.

$$R_d \geq Q_d \tag{1}$$

Each design code specifies different sets of factors for assessing design resistance R_d. In addition, the factors for evaluating the design load effect (Q_d) rely on the *load and action* codes associated

*Corresponding author. *E-mail address:* vanson.ctt@vimaru.edu.vn (Doan, N. S.)

with the design codes used. For example, when using AISC 360-16 [4] to design steel structures, ASCE/SEI 7-16 [5] is adopted to assess the load effects. Alternatively, EC 0 and EC 1 are utilized to determine the load effects when EC 3 is selected for designing steel structures [6, 7].

In LSD, successful design solutions are those satisfying the design equation (Eq. (1)) using factor sets provided in the design codes and the load and action codes. In design practices, the optimal solution can be achieved by designing such that the limit states (equal sign in Eq. (1)) are achieved for all members. For instance, in the case of truss structures, members are selected such that resistances of tension and compression bars are enough for carrying the applied loads but not significantly larger than the load effects. Assuming that the idea of designing at the limit states is all achieved using the two design codes, it is difficult to conclude which design solution is the more reasonable solution than another. In contrast, using probabilistic analyses, the more reasonable design solutions can be identified by those having a more consistent and uniform safety level of all members. For instance, the more suitable design of truss structures might have a reasonable uniformity of safety levels considering both tension and compression bars. In contrast, the trusses with significant differences in tension and compression safety levels are not appropriate design solutions.

To address the challenge of comparing design solutions designed by different LSD codes, this study conducts probabilistic analyses to assess the probabilistic safety levels of the truss members designed with the ultimate (or strength) limit states in the two design codes. Based on the probabilistic results obtained, the more consistent and uniform designs can be identified, as aforementioned. The LSDs of truss members are first summarized in Section 2 for the two design codes. Then, Section 3 briefly presents the Monte Carlo simulation (MCS) applied to truss problems. The two truss structures examined in this work are presented in Section 4. Because comparing two design codes is an ambitious goal, this study is limited to the planar trusses and ultimate limit states applied to truss bars. Section 5 shows the results of the limit state design and the corresponding probabilistic results evaluated for each LSD solution. Furthermore, six ratios of live-to-dead loads are employed to examine their effects on the probabilistic results in Section 5. Finally, conclusions are summarized in Section 6.

2. Limit state design for truss members using AISC 360-16 and EC 3

The truss structure is focused on in this work; hence, the tension and buckling capacities of the truss members are presented in this section. When using AISC 360-16, the load effects are determined based on ASCE 7-16. Alternatively, when using EC 3, the load and action code of EC 1 is employed, as presented previously. For convenience, the use of the American codes and European standards can be shortened by using AISC and EC in this work. The design equations corresponding to AISC and EC can be written as Eqs. (2a) and (2b) for steel truss members. Noticeably, AISC uses the load and resistance factors, while EC adopts a partial safety factor format for design equations.

$$\phi_R R_n \geq \sum \gamma_i Q_{n,i} \tag{2a}$$

$$\frac{R_k}{\gamma_M} \geq \sum \gamma_i Q_{k,i} \tag{2b}$$

In the equations, R and Q denote resistance and load components, respectively. Subscript k indicates characteristic values used in EC, whereas n denotes nominal values when using AISC. ϕ_R is the resistance factor specified in AISC 360-16 to account for uncertainty in computing capacity, which shares the same physical meaning with the partial safety factor for material properties (γ_M) adopted in EC 3. The two design codes combine the load effects by accounting for the load factor γ_i (for the i^{th} load). Various load combinations are recommended in the two load and action codes. For strength

limit states, the two combinations in Eqs. (3a) and (3b) can be used to determine the load effects corresponding to AISC and EC, respectively.

$$Q_n = 1.20D + 1.60L \tag{3a}$$

$$Q_k = 1.35D + 1.50L \tag{3b}$$

In Eq. (3), D and L denote the responses of structures against the dead and live load, respectively. It is clearly seen in Eq. (3) that different load effects will be determined for different codes, even though the same nominal (or characteristic) values of the dead and live load are applied to the same structure. For comparison purposes, the same values of the combined loads are used in this work when using the two design codes.

The tension resistances of the truss members are calculated based on the gross section (A_g), as shown in Eqs. (4a) and (4b), corresponding to AISC 360-16 and EC 3, respectively.

$$R_t^{AISC} = \phi f_y A_g \tag{4a}$$

$$R_t^{EC} = \frac{f_y A_g}{\gamma_{M_0}} \tag{4b}$$

In Eq. (4), f_y is the yield strength of steel material. For tension resistance, a resistance factor (ϕ) of 0.9 is taken as per AISC, while a partial safety factor (γ_{M_0}) of 1.0 is specified in Section 6 of EC 3.

Following AISC 360-16, the buckling resistance is determined based on the flexural buckling stress F_{cr}, as shown in Eq. (5). Resistance factor ϕ is also specified by 0.9, like the tension bar per AISC 360-16.

$$R_b^{AISC} = \phi F_{cr} A_g \tag{5}$$

The flexural buckling stress F_{cr} is determined based on the slenderness of member (λ), as shown in Eqs. (6a) or (6b) below:

$$F_{cr} = \left(0.658^{\frac{f_y}{F_e}}\right) f_y \quad \text{when} \quad \lambda \leq 4.71\sqrt{E/f_y} \tag{6a}$$

$$F_{cr} = 0.877F_e \quad \text{when} \quad \lambda > 4.71\sqrt{E/f_y} \tag{6b}$$

where $\lambda = \dfrac{KL}{r}$ and $F_e = \dfrac{\pi^2 E}{\lambda^2}$. L and r correspond to the length of the element and radius of gyration of the section, and K is the effective length factor.

For EC 3, the buckling resistance of compression members is assessed by Eq. (7).

$$R_b^{EC} = \frac{\chi A_{eff} f_y}{\gamma_{M_1}} \tag{7}$$

In Eq. (7), χ is the reduction factor, which is dependent on buckling mode and evaluated by Eq. (8).

$$\chi = \frac{1}{\Phi + \sqrt{\Phi^2 - \overline{\lambda}^2}} \tag{8}$$

where $\Phi = 0.5\left[1 + \alpha\left(\overline{\lambda} - 0.2\right) + \overline{\lambda}^2\right]$. The non-dimensional slenderness $\overline{\lambda}$ is calculated by Eq. (9), wherein $\lambda_1 = \pi\sqrt{E/f_y}$.

$$\overline{\lambda} = \lambda\frac{\sqrt{\frac{A_{eff}}{A_g}}}{\lambda_1} \tag{9}$$

In the equations, A_{eff} and A_g denote areas of the effective section (when buckling) and gross section, respectively. α is the imperfection factor, depending on the type of cross sections. γ_{M_1} is the partial safety factor of steel materials under flexural buckling conditions. Similar to tension members, EC 3 also specifies γ_{M_1} equal to 1.0 for buckling checking of compression bars. The effective area (A_{eff}) depends on the classifications of the sections, depending on the width-to-thickness ratios of sections, and are summarized in Table 5.2 of the code. For the first three classes, the effect area will be taken as the gross area.

3. Reliability analysis for truss structure

The reliability analyses carried out in this work aim to assess the probabilistic safety levels of the trusses designed by the two design codes. Based on the probabilistic results, comparisons can be easily made for design solutions using the two codes.

Three methods of reliability analyses can be commonly implemented, including the mean value first-order second-moment, the first-order reliability method, and MCS [8–10]. Because the first two methods require explicit fashions of the limit state equations, and this study handles the implicit structural problems, the MCSs are preferably applied [10–13]. The MCS helps simulate sets of sampling points of uncertain variables. Afterward, the deterministic calculations are repeatedly performed for each sample to assess the limit state equation. The number of failure events among all realizations is recorded to determine the failure probability. The failure probability and the associated reliability index can be calculated by Eqs. (10) and (11), respectively.

$$P_f = \frac{N_{failure}}{N} \tag{10}$$

$$\beta = \Phi^{-1}\left(1 - P_f\right) \tag{11}$$

In the equation, $N_{failure}$ and N correspond to the number of failure events and the size of MCS. Φ^{-1} is the inverse standard normal distribution. The limit state equation can be written as Eq. (12) for the two strength limit states of truss bars [10].

$$g = FS - 1 = \frac{R}{Q} - 1 \tag{12}$$

The uncertainties involved in the steel truss structures consist of material properties of steel members such as yield strength (f_y), Young's modulus (E), and cross-sectional properties such as areas or thicknesses of the sections. Normal distributions are utilized for these uncertain [10, 14–17]. Two typical loads, including the dead and live load (variable actions in EC), are used in this work. The dead load applied to structures is simulated as a normal distribution with a mean of 1.05 and COV of 10%. Meanwhile, Extreme type 1 distribution is utilized for live load as recommended in most previous studies [10, 16–18]. All uncertain variables (represented by their bias factors) are summarized in Table 1. Various ratios of the live-to-dead loads are used to examine their effects on the probabilistic safety levels. This ratio is recommended for steel structures from 0 to 5.0, and six values, including 0, 0.5, 1.0, 1.5, 3.0, and 5.0, are examined in this work. The larger-than-unity ratios are utilized to reflect the fact that the live load tends to be larger than the dead load in steel structures [16].

Table 1. Random variables considered

No.	Symbol	Description	μ	COV	Distribution
1	t	Thickness of sections (mm)	0.964	0.04	Normal
2	E	Young's modulus (MPa)	1.00	0.06	Normal
3	F_y	Yield strength (MPa)	1.10	0.10	Normal
4	D_i	Dead load (kN)	1.05	0.10	Normal
5	L_i	Live load (kN)	1.00	0.25	Extreme type 1

Note: The subscript i denotes the i^{th} loads (D or L) applied to the truss.

Generally, to evaluate axial forces in truss members, the finite element method (FEM) is commonly adopted [19]. Several machine-learning approaches have recently been investigated to develop surrogate models for truss structures [20]. Based on the surrogate models, the computing time can be essentially reduced for complicated structures; however, there are still errors in the predictions of the surrogate models (e.g., an error of 6%, as presented in [20]). In this work, the *FEM-Truss*, a MATLAB program developed in the previous work [10], is employed to assess the axial forces of truss members accurately. One million samples, recommended for the size of MCSs with an expected reliability index of 3.9 in previous work [10], are also used in the present study.

4. Case studies of two planar trusses

In this work, two truss profiles are examined, as shown in Fig. 1. The first truss, Truss 1 shown in Fig. 1(a), is a simply supported truss consisting of 23 members. This truss was investigated in previous works [10, 17], and it was reported that the compression reliability index is higher than that for tension members. However, only AISC 360-16 and a live-to-dead load ratio of 3.0 was examined in their studies. The members of Truss 1 are classified into three groups, including the upper chord, lower chord, and the web members. The squared hollow sections provided by SSAB Domex Tube (available on www.ssab.com for steel sections) are employed to design sections. The web members are not critical bars, and they are chosen as 120 × 5.6 mm. The chord members (tension and compression bars denoted by T and C in Fig. 1) are designed in this work using the two design codes, as presented in

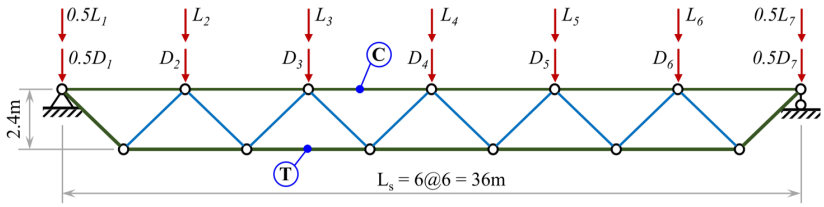

(a) A simply supported truss (Truss 1)

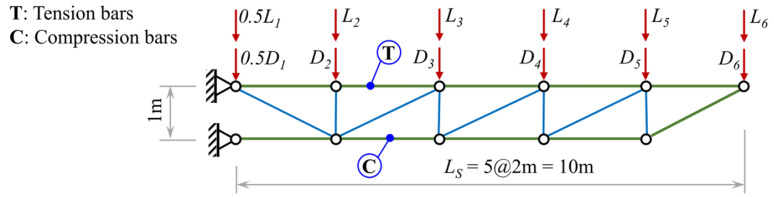

(b) A cantilever truss (Truss 2)

Figure 1. Truss problems

Section 2. The deterministic and probabilistic results will be presented in Section 5. Notably, Truss 1 involves 19 uncertain variables.

The second truss, Truss 2, is a cantilever structure with a span length and a truss height of 10m and 1 m, respectively. This truss consists of 14 members and carries six dead loads and live loads applied to the nodes in the upper chord, as shown in Fig. 1(b). Similar to Truss 1, the chord bars are also designed following the two design codes. The web members are chosen as 120 × 5.6 mm. Noticeably, the same models of uncertainties summarized in Table 1 are applied to the two trusses.

For a fair comparison, the same values of combined loads are used for designing truss members. Namely, 90 kN and 62 kN combined loads are applied to Truss 1 and Truss 2, respectively. Notably, different ratios of live-to-dead load are considered, but the combined loads are constantly kept in this work, and the nominal values will vary for each ratio considered. Using these combined loads, the axial forces in the truss members are presented in Fig. 2 for the two trusses. Considering the maximum tension and compression forces for each truss, the same sections will be designed for each behavior using the two design codes, and the results will be presented in Section 5.

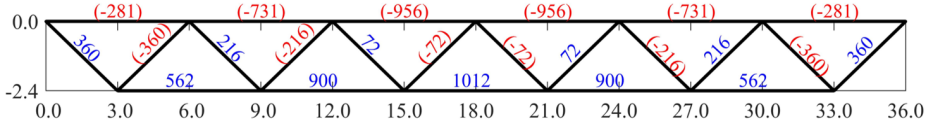

(a) For Truss 1

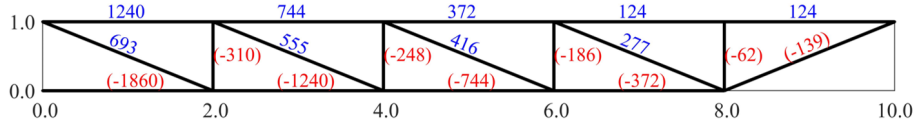

(b) For Truss 2

Figure 2. Resultant axial forces (1.20D+1.60L using ASCE/SEI 7-16 and 1.35D + 1.50L using EC 0)

5. Results and discussions

In this section, feasible sections will be designed for tension and compression members of each truss to ensure the limit state equations presented in Subsection 5.1 for the two design codes. The width of squared hollow sections ranges from 120 mm to 220 mm, while the thicknesses are selected from 3.0mm to 12.5mm as provided by the SSAB catalog. To ensure the limit state, i.e., remaining equals signs in the design equation (Eq. (2)), the sections are chosen such that the ratios of the design resistance and the combined load are not larger than 1.05. That means the redundancy of the design solutions is not higher than 5%, which will help comparisons of the limit-state design solutions following different design codes more suitable. The deflections of trusses are also checked to ensure the limits of $L_s/300$ for Truss 1 and $L_s/150$ for Truss 2 using AISC [4]. When using EC 3, deflection limits of $L_s/360$ and $L_s/180$ are employed for Truss 1 and Truss 2, respectively [6]. The MCSs are then executed and reported in Subsection 5.2 for each design solution of each truss, as presented in Section 3. The reliability index will be used for comparing purposes concerning the probabilistic point of view.

5.1. Results and discussion on deterministic designs

Considering the maximum axial forces reported in Fig. 2, the results of tension checks for Truss 1 are reported in Figs. 3(a) and 3(b), corresponding to AISC and EC. For compression bars, Figs. 4(a) and 4(b) show feasible sections using AISC and EC, respectively. Similarly, Figs. 5(a) and 5(b) summarize the tension capacities of sections for Truss 2, corresponding to AISC and EC. Figs. 6(a)

and 6(b) present the sections found for compression members of Truss 2 associated with AISC and EC, respectively.

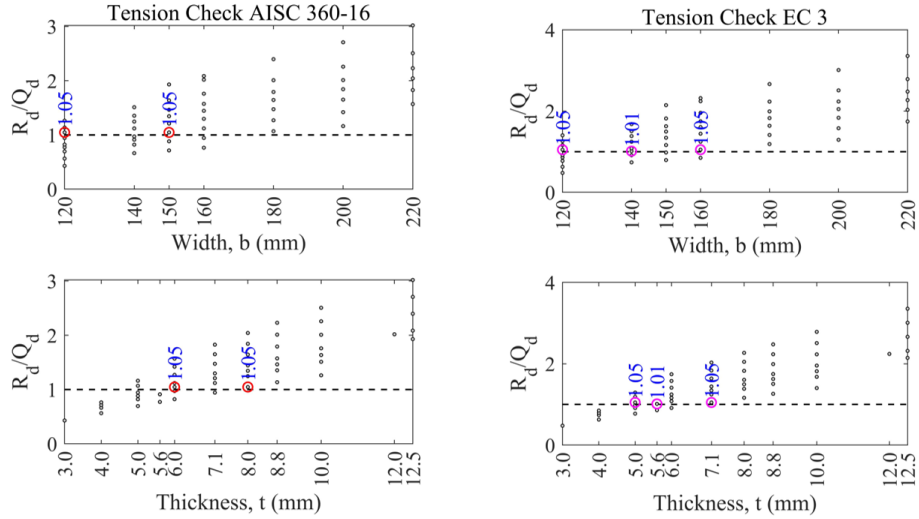

(a) Using AISC (b) Using EC

Figure 3. Tension verifications for Truss 1

The dashed lines in the figures indicate the limit states, i.e., the equal sign in the design equations. The feasible sections, i.e., the sections that succeed in the verification but have a redundant capacity within 5%, are shown by circle markers in the figures. It is worth noting that the same results can be obtained in deterministic designs for every load ratio because the same combined loads are utilized.

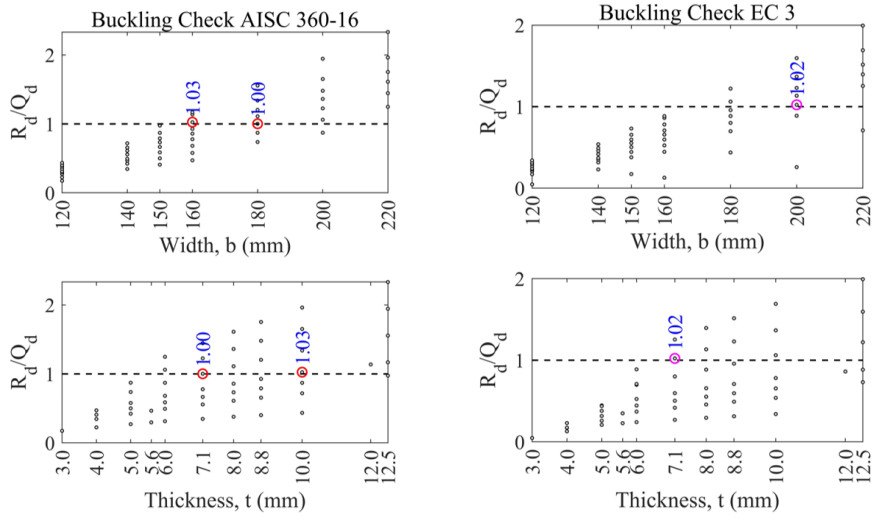

(a) Using AISC (b) Using EC 3

Figure 4. Compression verifications for Truss 1

Figs. 3 and 4 indicate that the two sections, including 120 × 8.0 mm and 150 × 6.0 mm, can be chosen for tension bars of Truss 1 when using AISC. When using EC 3, three sections, including 120 × 7.1 mm, 140 × 5.6 mm, and 160 × 5.0 mm, are desired for the tension checks and fall in 5% of the

redundancy. For compression bars of Truss 1, two sections of 160 × 10.0 mm and 180 × 7.1 mm are suitable when using AISC; meanwhile, when using EC, only one section of 200 × 7.1 mm is suitable for Truss 1.

Among 54 sections investigated for Truss 2, three sections are suitable for tension bars when using AISC (120 × 10.0 mm, 140 × 8.0 mm, and 180 × 6.0 mm), as reported in Fig. 5(a). If EC is employed, three sections, 120 × 8.8 mm, 140 × 7.1 mm, and 160 × 6.0 mm, can be used for tension members. For compression, two sections (160 × 12.0 mm, 180 × 10.0 mm) can be designed when using AISC. When using EC, two sections, including 200 × 8.0 mm and 220 × 7.1 mm, are feasible for compression bars of Truss 2. The number of feasible sections for each behavior and each design code are recorded in Table 2. More details for each design solution will be presented later.

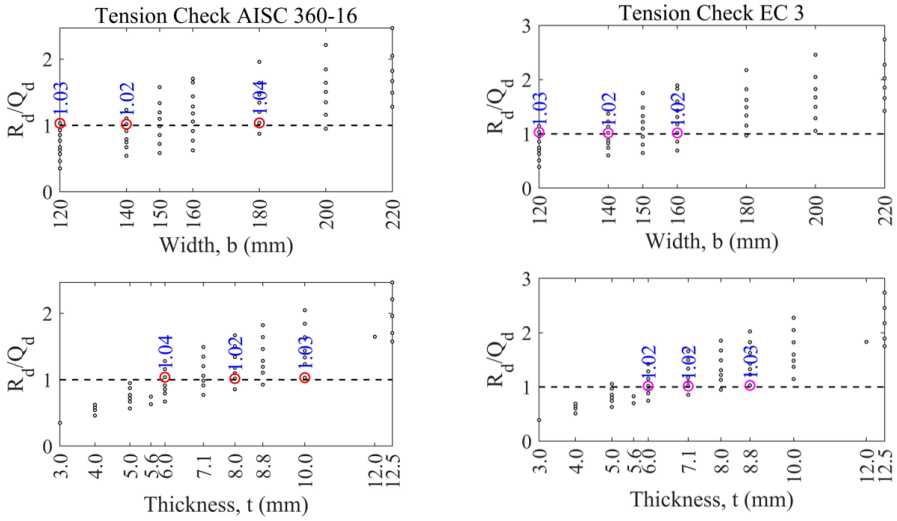

(a) Using AISC (b) Using EC 3

Figure 5. Tension verifications for Truss 2

Table 2. Feasible sections for the two truss structures regarding two design codes

Behavior	Truss 1		Truss 2	
	AISC	EC	AISC	EC
Tension	(2) 120 × 8.0 150 × 6.0	(3) 120 × 7.1 140 × 5.6 160 × 5.0	(3) 120 × 10.0 140 × 8.0 180 × 6.0	(3) 120 × 8.0 140 × 7.1 160 × 6.0
Compression	(2) 160 × 10.0 180 × 7.1	(1) 200 × 7.1	(2) 160 × 12.0 180 × 10.0	(2) 200 × 8.0 220 × 7.1

Table 2 indicates that larger sections are required for all tension members of the two trusses when using AISC, compared to using EC. For instance, a thickness of 8.0 mm is needed for the same width section of 120 mm when using AISC, whereas a thickness of 7.1 mm is needed for tension members using EC. In contrast, Table 2 also reveals that larger sections are required for compression members designed by EC, compared to AISC. For example, a wider section of 200 × 7.1 mm is needed for

compression members of Truss 1 when using EC, but a smaller section of 180 × 7.1 mm is needed for the same compression member when using AISC.

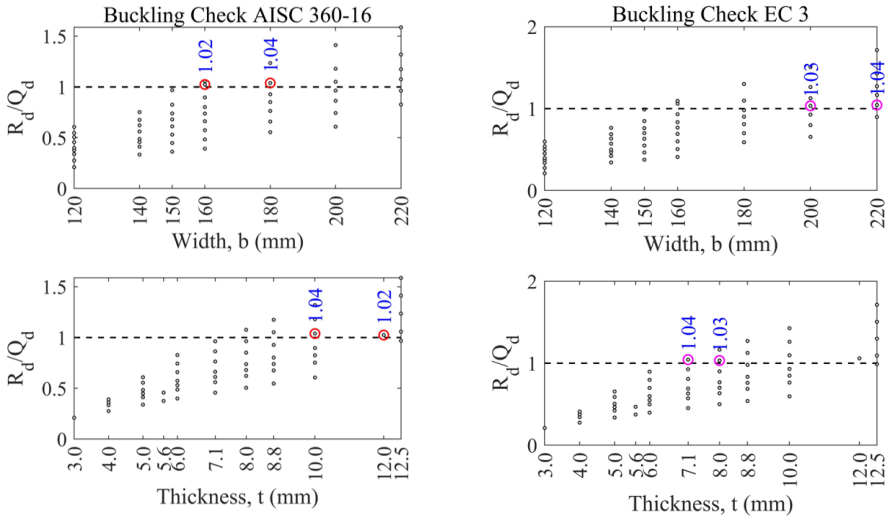

(a) Using AISC (b) Using EC 3

Figure 6. Compression verifications for Truss 2

5.2. *Results and discussion on probabilistic analyses*

This subsection presents the results obtained from MCSs for 18 cases reported in Table 2. It should be recalled that six ratios of the live-to-dead loads are examined in this work for each truss and each design code; hence, each case shown in Table 2 will be carried out six times. Consequently, 108 cases are involved in the probabilistic analyses. For illustration purposes, the load ratio of 1.5 is presented in Figs. 7 to 10 for the two trusses. Finally, the results for all cases are summarized in Figs. 11 and 12.

Namely, Figs. 7 and 8 show the MCS results for tension and compression behaviors of Truss 1, respectively. Likewise, Figs. 9 and 10 report the probabilistic results for Truss 2. In the figures, the left panels present the histograms of load and resistance realizations obtained from MCSs, while the right panels illustrate the safety factors (i.e., the ratios of resistance R and load Q). The statistical properties, including the mean (μ) and the coefficients of variation (COV), are also captured in the figures.

It is seen in the figures that the reliability indexes for design solutions (both tension and compression) following AISC are higher than those using EC. Notably, the same phenomenon is also observed for the compression bars, wherein the section designed using EC is even larger than that using AISC, as presented in Subsection 5.1. It should be mentioned that the COVs of the safety factor (R/Q) are relatively similar for the same behavior regardless of the code used. Meanwhile, the means of the FSs show some differences. Considering tension members of Truss 1 in Fig. 7, for example, the same COVs of 0.130 are obtained for the FSs when using the two design codes. Meanwhile, the mean value of FS realization using AISC (1.751) is higher than that using EC (1.578). Consequently, the reliability indexes obtained from AISC might be higher than those using EC because the reliability index positively correlates to the FSs.

It is also observed in the figures that the same statistical properties of the loads are obtained regardless of the codes used. Considering the same behavior (i.e., tension or compression), COVs

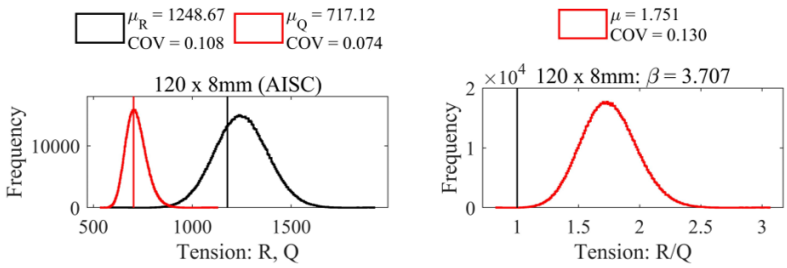

(a) By AISC

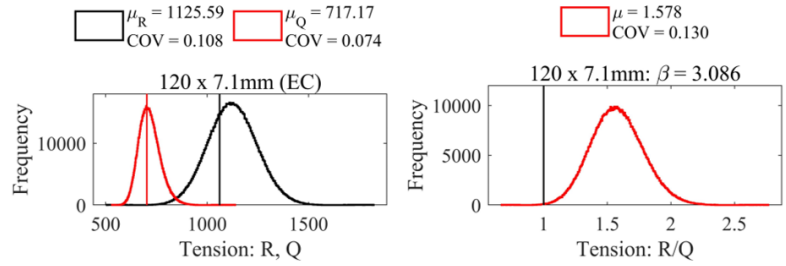

(b) By EC

Figure 7. MCS results of tension bars of Truss 1 designed

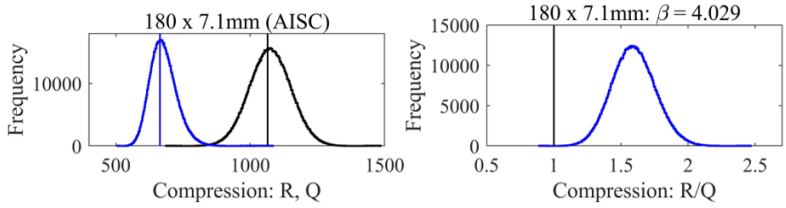

(a) By AISC

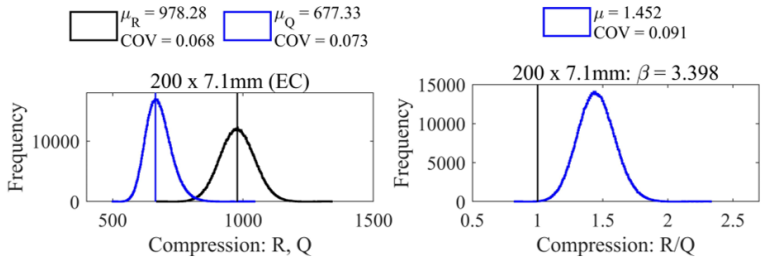

(b) By EC

Figure 8. MCS results of compression bars, Truss 1 designed

of resistance realizations are quite similar for the two design codes, and the most differences are shown by means of the resistances. These observations explain why the mean safety factors (which are calculated by the ratios of resistances and loads) are not identical using the two design codes. Notably, the two determinate trusses are investigated, and the same combined loads are utilized; therefore, the same statistical properties of the loads might be obtained. Differences in the safety factors are attributed to the means of resistance components that are differently estimated as per design codes. For example, the larger section obtained from AISC results in a higher mean of the tension resistance,

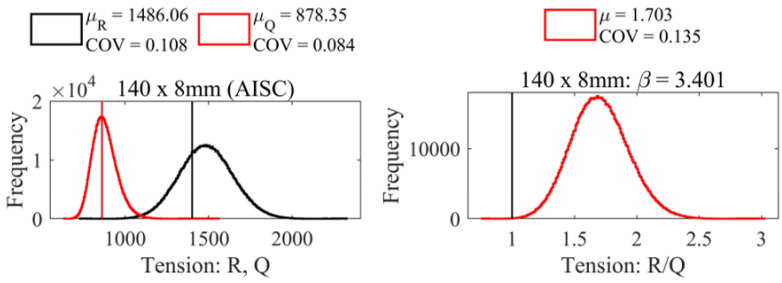

(a) By AISC

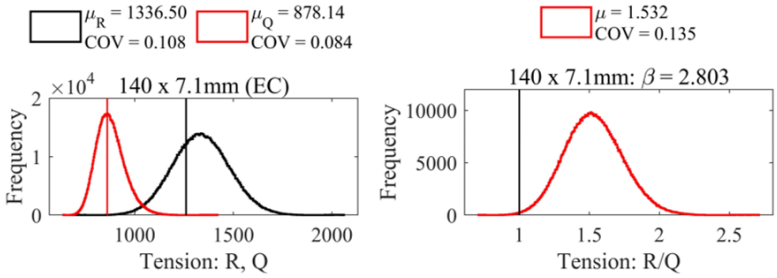

(b) By EC

Figure 9. MCS results of tension bars of Truss 2 designed

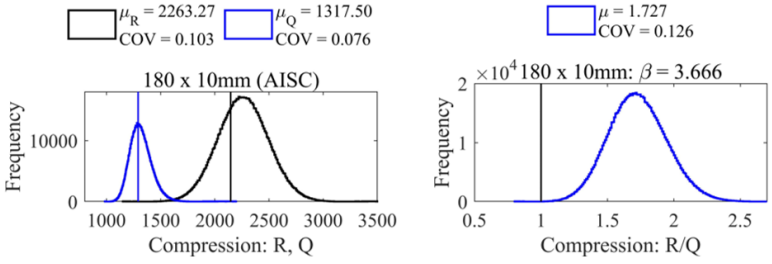

(a) By AISC

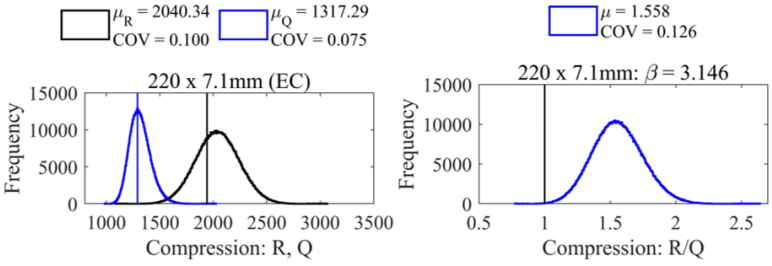

(b) By EC

Figure 10. MCS results of compression bars, Truss 2

as depicted in Fig. 7. For compression behaviors and considering the same either sections or effective lengths of members, compression resistances estimated by AISC are higher than those using EC. This statement is evidenced by Fig. 4(b), wherein the wider section is required for EC (200 mm) compared to that designed by AISC (180 mm), although the same thickness of 7.1 mm is utilized.

Fig. 11 summarizes the probabilistic results estimated for all feasible cases reported in Table 2.

Notably, although the same sections are designed by deterministic calculations for all load ratios, different nominal dead loads (D_n) and live loads (L_n) are used in probabilistic analyses to keep the same factored loads. Consequently, probabilistic results might depend on load ratios, as illustrated in Fig. 11.

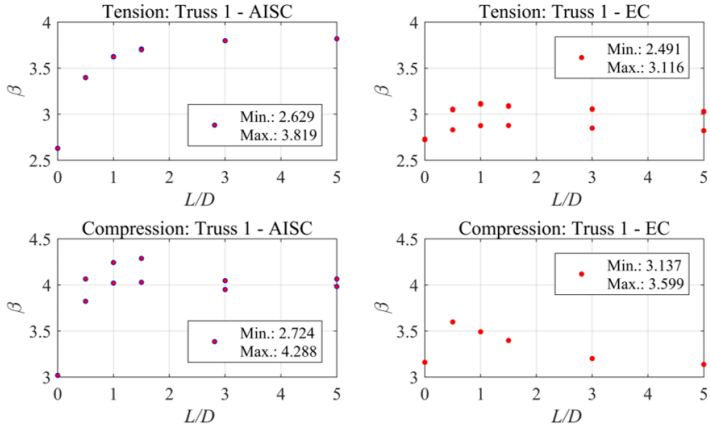

(a) For Truss 1

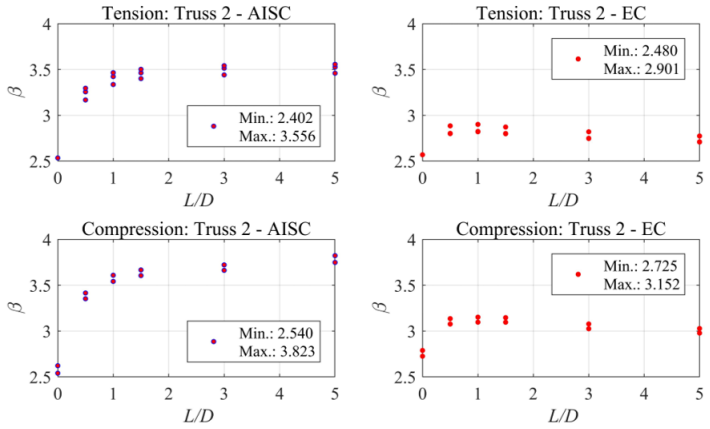

(b) For Truss 2

Figure 11. MCS results for all ratios of live-to-dead load

The results in Fig. 11 indicate that the design solutions using AISC generally achieve higher probabilistic safety levels for both tension and compression behaviors, although the same uncertain models are adopted. For instance, tension reliability indexes for Truss 1 vary from 2.629 to 3.819 when using AISC. Meanwhile, a lower range of reliability indexes (from 2.491 to 3.116) is obtained for the tension members designed by EC. For compression behaviors, higher reliability indexes are also obtained for design solutions using AISC compared to those using EC. Furthermore, Fig. 11 illustrates that the probabilistic safety levels are consistently achieved for the two behaviors when designed by EC. Contrastingly, larger gaps between the tension and compression safety levels are observed for the two trusses designed by AISC.

To understand the lower reliability indexes reported for the designs using EC, Fig. 12 summarizes the nominal safety factors (depicted by the ratios of nominal resistances and nominal loads) for all design solutions using the two design codes. It is observed in the figure that the nominal safety factors

of designs using AISC are higher than those using EC. It should be recalled that the same means and COVs of the loads and the relative similarity for COVs of the resistances are achieved when using the two design codes, as presented in Figs. 9 and 10. Therefore, the differences in the nominal safety factors reported in Fig. 12 are attributed to the differences in estimations of the nominal resistance using the two design codes.

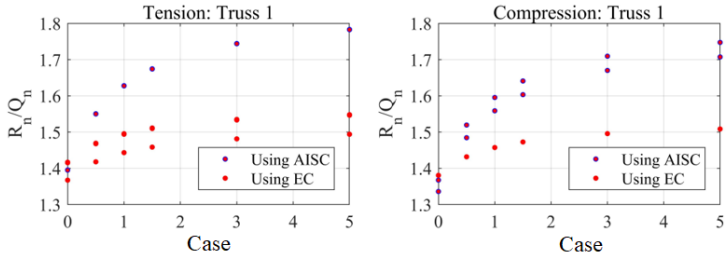

(a) For Truss 1

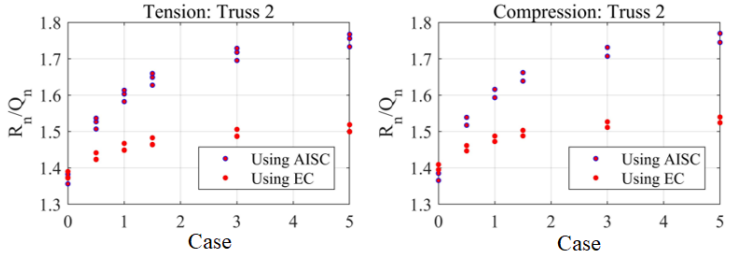

(b) For Truss 2

Figure 12. Comparison of nominal safety factor (R_n/Q_n) for all load ratios

6. Conclusions

This study assesses the probabilistic safety levels of two truss structures that are designed using the two LSD codes of AISC 360-16 and EC 3. The procedures of the LSDs are first adopted to design tension and compression members of two truss structures. Afterward, Monte Carlo simulations are executed to evaluate the failure probabilities and the associated reliability indexes of the design solutions. The two planar trusses and ultimate limit states are focused on this work. Future studies can be examined for problems relating to 3D trusses or connections. Based on the limit state designs and the probabilistic assessments obtained in this work, several conclusions are revealed.

From the limit state designs, larger sections are required for tension members designed by AISC, compared to those using EC. Nonetheless, compression bars satisfying AISC provisions are smaller than those designed by EC.

The probabilistic results obtained in this work reveal that the same coefficient of variations are obtained for load and resistance, which indicates that the same uncertain levels of resultants are applied to the same truss regardless of the codes used. Nevertheless, significant differences are observed for the means of resistances that cause variations in the probabilistic safety levels of the design solutions using the two design codes.

108 MCSs are executed for 18 LSD solutions and six different load ratios regarding two truss structures. The results obtained from the simulations indicate that the probabilistic safety levels of both tension and compression members designed by AISC are generally higher than those using EC. Moreover, larger gaps between the reliability indexes estimated for tension and compression behaviors

are reported for trusses designed by AISC compared to those using EC. That is, the uniformity and consistency of reliability indexes are for trusses designed by EC.

Acknowledgments

This research is funded by Vietnam Maritime University under grant number: DT23-24.81.

References

[1] Dinh, H.-B., Mac, V. H., Doan, N. S. (2024). Comparative study on semi-probabilistic design methods to calibrate load and resistance factors for sliding stability design of caisson breakwaters. *Ocean Engineering*, 293:116573.

[2] Arrayago, I., Zhang, H., Rasmussen, K. J. R. (2022). Simplified expressions for reliability assessments in code calibration. *Engineering Structures*, 256:114013.

[3] Duong, B., van Gelder, P. (2016). Calibrating resistance factors under load and resistance factor design method (LRFD) using Monte-Carlo simulation. *Journal of Science and Technology in Civil Engineering (STCE)-NUCE*, 10(5):79–87.

[4] AISC 360-16 (2016). *Specification for Structural Steel Buildings*. American Institute of Steel Construction: Chicago, USA.

[5] ASCE/SEI 7-16 (2016). *Minimum Design Loads for Buildings and Other Structures*. American Society of Civil Engineers: Reston VA, USA.

[6] Gardner, L. (2011). *Designers' Guide to Eurocode 3: Design of Steel Buildings*. 2nd edition, Thomas Telford Ltd.

[7] EC 3 (2005). *Design of Steel Structures, Part 1-1: General Rules and Rules for Buildings*. Brussels, Belgium.

[8] Nowak, A. S., Collins, K. R. (2012). *Reliability of Structures*. 2nd edition, CRC Press.

[9] Doan, N. S., Huh, J., Mac, V. H., Kim, D., Kwak, K. (2020). Probabilistic Risk Evaluation for Overall Stability of Composite Caisson Breakwaters in Korea. *Journal of Marine Science and Engineering*, 8(3): 148.

[10] Doan, N. S. (2023). A study on the probabilistic safety assessment of the truss structure designed by the LRFD code. *Journal of Science and Technology in Civil Engineering (STCE) - HUCE*, 17(1):111–124.

[11] Doan, N. S., Dang, P. V., Huh, J., Mac, V. H., Haldar, A. (2022). Efficient approach for calibration of load and resistance factors in the limit state design of a breakwater foundation. *Ocean Engineering*, 251: 111170.

[12] Doan, N. S., Huh, J., Mac, V. H., Kim, D. H., Kwak, K. (2021). Calibration of Load and Resistance Factors for Breakwater Foundations under the Earthquake Loading. *Sustainability*, 13(4):1730.

[13] Doan, N. S. (2023). Reliability analysis and uncertainty quantification of clay and sand slopes stability evaluated by Fellenius and Bishop's simplified methods. *International Journal of Geo-Engineering*, 14 (1).

[14] Ellingwood, B., Galambos, T. V., MacGregor, J. G., Cornell, C. A. (1980). *Development of a probability based load criterion for American National Standard A58*. 1st edition, National Bureau of Standards. Special Publication No. 577: Washington D. C., USA.

[15] Galambos, T. V., Ravindra, M. K. (1981). Load and resistance factor design. *Engineering Journal, American Institute of Steel Construction*, 18(3):78–84.

[16] Zhang, H., Liu, H., Ellingwood, B. R., Rasmussen, K. J. R. (2018). System Reliabilities of Planar Gravity Steel Frames Designed by the Inelastic Method in AISC 360-10. *Journal of Structural Engineering*, 144 (3).

[17] Blum, H. B. (2013). *Reliability-Based Design of Truss Structures by Advanced Analysis*. Research Report R936, The University of Sydney, Sydney, Australia.

[18] Ellingwood, B., Galambos, T. V. (1982). Probability-based criteria for structural design. *Structural Safety*, 1(1):15–26.

[19] Logan, D. L. (2011). *A first course in the finite element method*, volume 4. Thomson, London, UK.

[20] Hung, D. V., Phu, N. T. (2023). Towards a generalized surrogate model for truss structure analysis using graph learning. *Journal of Science and Technology in Civil Engineering (STCE) - HUCE*, 17(2):99–109.